



# Germanium iodide mediated synthesis of nanodiamonds from adamantane “seeds” under moderate high-pressure high-temperature conditions

Jiaxu Liang, Christopher P. Ender, Todd Zapata, Anna Ermakova, Manfred Wagner, Tanja Weil\*

Max Planck Institute for Polymer Research, Ackermannweg 10, Mainz 55128, Germany

## ARTICLE INFO

### Keywords:

Nanodiamonds  
Moderate high-pressure high-temperature  
Germanium iodide  
Bottom-up diamond synthesis

## ABSTRACT

There is an emerging demand for nanodiamonds with controlled structures or shapes for applications in biomedical imaging and sensing. Synthetic conditions proceeding at less harsh temperatures and pressures are considered crucial to control nanodiamond formation process. We report a germanium iodide ( $\text{GeI}_4$ ) mediated synthesis of nanodiamonds from diamondoid molecules and alkane hydrocarbon under moderate high-pressure high-temperature (m-HPHT) conditions. For the first time,  $\text{GeI}_4$  is used to generate nanodiamonds at 3.5 GPa and 500 °C, which is considerably lower than the conditions reported for common HPHT methods for nanodiamond synthesis. The strategy reported herein allows synthesizing nanodiamonds based on well-defined molecular precursors, which paves the way to a bottom-up diamond synthesis designed at a molecular level.

## 1. Introduction

The unique properties of nanodiamonds make them a promising material for various applications such as biomedical imaging and sensing [1]. Nanodiamonds are biocompatible and chemically robust due to their  $\text{sp}^3$  bonded carbon lattice. More importantly, some atomic defects in the lattice known as color centers exhibit emission from the visible to the near-infrared light with high photostability, and they can serve as fluorescent biomarkers and nanoscale sensors [2]. The properties are strongly affected by the structures of the nanodiamonds. For instance, the type of color center determines the emission spectrum; the brightness of the fluorescent nanodiamonds depends on the average number of emitting color centers per particle, and the color center stability is associated with the sizes of the nanoparticles and their surface chemistries [3]. Thus, it is of great importance to control their sizes, shapes and defects in a reproducible fashion. Common methods of nanodiamond synthesis such as detonation [4], laser ablation [5] and chemical vapor deposition (CVD) [6] proceed either under non-equilibrium conditions or the pressure and temperature are insufficiently controlled, thus limiting the control of the final products' structures [1,7]. Alternatively, the high-pressure high-temperature (HPHT) technique holds great promise by providing pressure and temperature control over a wide range. It has been demonstrated that the precursors have an important impact on the structures of the final products under HPHT conditions [8]. Graphite is a conventional precursor, which requires harsh conditions (over 10 GPa and 2000–3000 °C) for direct

conversion to diamond [9]. If non-graphitic carbon materials, like amorphous carbon or glassy carbon, are used as starting materials, conversion to diamond occurs at lower temperatures (1600–1800 °C) [10]. By applying different catalytic medium, the synthetic conditions have been reduced to 5–7 GPa and 1300–1500 °C [11–13]. Recently, hydrocarbons such as diamondoids have been demonstrated as promising precursor molecules, and it was speculated that the presence of  $\text{sp}^3$ -hybridized carbon in their structure promotes the formation of diamond [14]. A diamondoid molecule resembles part of the hydrogen-terminated diamond lattice and could be considered as an ultrasmall diamond with a precisely defined structure. Therefore, seeded growth based on diamondoid molecules would enhance nucleation and yield much higher quality nanodiamonds [3]. Moreover, a molecular “seed” with preorganized defect atoms would be favorable for the controlled growth of specific color centers within diamond [3]. However, the vigorous HPHT reaction conditions with very high temperatures of above 1000 °C would decompose any organic precursors into pyrolysis intermediates thus limiting the possibilities for engineered diamond growth. Thus, less harsh, “moderate” HPHT (m-HPHT) synthesis conditions are considered a key step towards the controlled synthesis of nanodiamonds. Some studies demonstrated that low temperature is available for diamond synthesis [15,16]. However, the pressure they use was still as high as 10 GPa and no *in situ* investigation was performed to study the chemical change inside the sample during the reaction.

Herein, we present the synthesis of nanodiamonds using

\* Corresponding author.

E-mail address: [weil@mpip-mainz.mpg.de](mailto:weil@mpip-mainz.mpg.de) (T. Weil).

<https://doi.org/10.1016/j.diamond.2020.108000>

Received 13 February 2020; Received in revised form 10 June 2020; Accepted 23 June 2020

Available online 06 July 2020

0925-9635/ © 2020 The Authors. Published by Elsevier B.V. This is an open access article under the CC BY-NC-ND license

(<http://creativecommons.org/licenses/by-nc-nd/4.0/>).

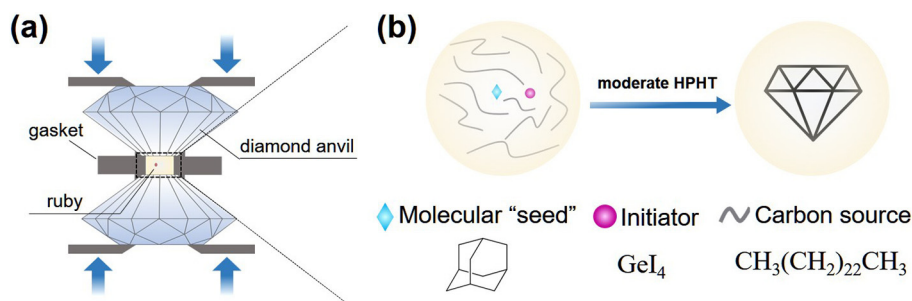


**Fig. 1.** Illustration of the  $\text{GeI}_4$ -mediated synthesis of nanodiamonds under m-HPHT conditions. (a) Schematic of the diamond anvil cell (DAC) setup. (b) Schematic of nanodiamond synthesis inside the sample chamber (as indicated by the dashed box) using adamantane as a molecular “seed”, tetracosane as alkane carbon source and  $\text{GeI}_4$  as an initiator.

adamantane as the “seed” and tetracosane as the carbon source under m-HPHT conditions (Fig. 1) in the presence of germanium iodide ( $\text{GeI}_4$ ). Adamantane has a molecular structure that resembles the diamond crystal lattice. It has been demonstrated that the diamondoid structure plays a key role in lowering nucleation barriers during diamond synthesis [17]. In some way, adamantane is able to act as a molecular “seed” to promote nucleation. The *in situ* Raman spectroscopy suggests that  $\text{GeI}_4$  can activate both adamantane and tetracosane to produce nanodiamonds at significantly lower pressure (3.5 GPa) and temperature (500 °C) compared to the conventional HPHT methods (normally 5–7 GPa and above 1000 °C). These results suggest that  $\text{GeI}_4$  could play a similar role in diamond HPHT synthesis as an initiator does in conventional organic reactions. Based on these new insights, we envision that diamond synthesis could be accomplished by classic organic chemistry methods thus opening up new opportunities for the bottom-up synthesis of nanodiamonds.

## 2. Experimental

The m-HPHT experiments were carried out in a diamond anvil cell (DAC) setup by placing the sample inside a gasket hole between the two anvils as a reaction chamber (as shown in Fig. 1a and supporting information). Pressure inside the chamber is generated by pressing the anvils and detected using ruby as the calibrant. The transparent diamond anvils also serve as windows for conducting *in situ* Raman spectroscopy and wide-field imaging. The sample consists of a mixture of  $\text{GeI}_4$ , adamantane and tetracosane with the molar ratio of 1:1:1000.

## 3. Results and discussion

*In situ* Raman spectroscopy records the evolution of the vibrational modes inside the sample during the reaction process. As shown in Fig. 2a, the Raman spectrum of the mixture of  $\text{GeI}_4$ , adamantane and tetracosane before heating shows the typical characteristics of alkanes with C–H stretching in the range of  $\sim 2700$ – $3100\text{ cm}^{-1}$  and C–C stretching as well as C–H bending modes at  $\sim 1000$ – $1300\text{ cm}^{-1}$  and  $\sim 1500\text{ cm}^{-1}$  [18]. These signals correspond to the Raman spectrum of pure tetracosane (see Fig. S1a), which was used in great excess. The *in*

*situ* Raman analysis gives important information about the chemical reaction during the m-HPHT cycle. At 500 °C, the intensities of the peaks at  $\sim 1000$ – $1500\text{ cm}^{-1}$  diminished and the peak width became wider due to the high temperature. A new peak at around  $1641\text{ cm}^{-1}$  appeared in the spectrum, which is associated with amorphous carbon. Since the strong Raman peaks from the diamond anvils overshadow the signals of any possible synthetic diamonds during the process, the formation of amorphous carbon becomes a good indicator for the reactivity of the precursors. Under these reaction conditions, tetracosane decomposes into smaller alkyl chains [19] that then either attach to adamantane for diamond growth or form amorphous carbon material through unsaturated aliphatic and alicyclic intermediates. After the reaction was quenched to room temperature, the amorphous carbon peak became even more evident and a broad photoluminescence background was observed. This strong photoluminescence background reveals a high hydrogen concentration in the amorphous carbon clusters [20]. The absence of clear D and G lines indicates that a large amount of  $\text{sp}^3$ -hybridized carbon species has formed. It has been demonstrated that hydrogenated diamond-like carbon normally forms together with diamond using diamondoid hydrocarbons as precursors in HPHT experiments [21], which also agrees with our experimental observations. Control experiments were performed with a mixture of adamantane and tetracosane without the  $\text{GeI}_4$ . The decrease in the peak intensity was also observed as shown in Fig. 2b. However, in this case, no peaks associated with the formation of amorphous carbon structures were detected in the Raman spectrum and only very minor changes in the fluorescence background occurred during the reaction. Therefore, the control experiment indicates that the mixture of adamantane and tetracosane is much less reactive in the absence of  $\text{GeI}_4$ . The same observations were reproduced in other control experiments with pure tetracosane and pure adamantane. In the presence of  $\text{GeI}_4$ , amorphous carbon peaks were observed after the heating cycles in both experiments (Figs. S1 and S2). These results indicate that  $\text{GeI}_4$  can function as an initiator, which enhances the chemical reactivity of both adamantane and tetracosane, thereby enabling the reaction already at moderate conditions.

After the m-HPHT reaction, the products were extracted with a tungsten carbide needle into 50  $\mu\text{L}$  of isopropanol alcohol and sonicated

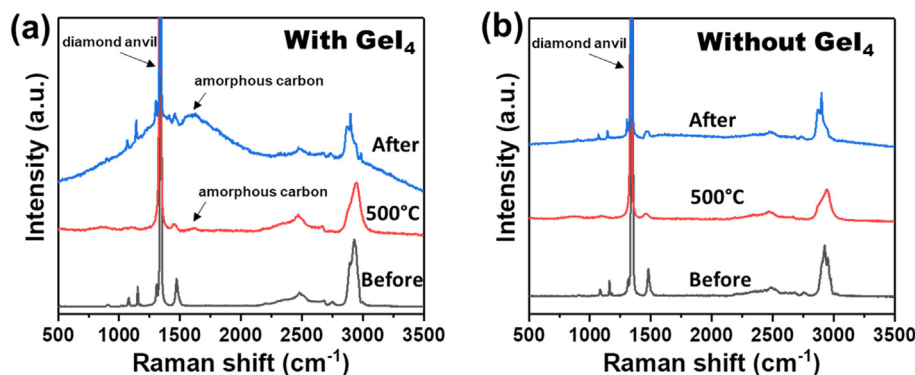


**Fig. 2.** *In situ* Raman spectra of the mixture of adamantane and tetracosane with (a) and without (b)  $\text{GeI}_4$  at 3.5 GPa before (black curves), during (red curves) and after (blue curves) heat treatment at 500 °C for 2 h. (For interpretation of the references to color in this figure legend, the reader is referred to the web version of this article.)

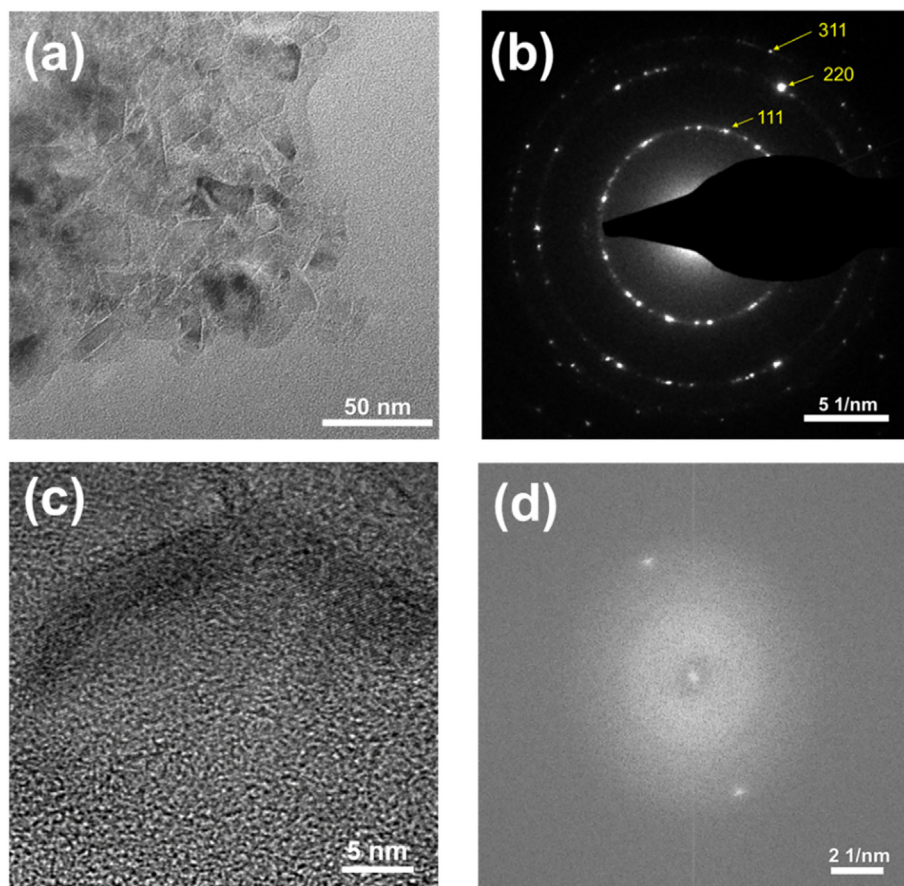


Fig. 3. TEM measurements of the product obtained after m-HPHT reaction of the mixture of  $\text{GeI}_4$ , adamantane and tetracosane. (a) TEM image of a diamond cluster observed in the product; (b) electron diffraction pattern exhibiting lattice spacings of 2.06, 1.27, and 1.08 Å corresponding to diamond (111), (220) and (311) planes; (c) a high resolution image; (d) fast Fourier transform calculated from image (c).

for 20 min for further characterization. The products obtained from the experiment with the mixture of  $\text{GeI}_4$ , adamantane and tetracosane were characterized by transmission electron microscopy (TEM). Clusters were found and their images were depicted in Fig. 3a. The particle sizes ranged from several nanometers to tens of nanometers. A rough estimation of the size distribution is shown in Fig. S3 with an average particle size of around 14.3 nm. The selected area electron diffraction pattern (Fig. 3b) showed reflections at 2.06, 1.27, and 1.08 Å corresponding to Miller indexes of (111), (220) and (311), thus indicating the diamond structure of these nanoparticles. Energy dispersive x-ray spectroscopy (EDX) in Fig. S4 reveals that carbon is the predominant element in the product, confirming that these reflections belong to diamond cell parameters rather than contaminations with similar crystalline structures. High resolution TEM image (Fig. 3c) revealed that the nanodiamonds were covered by organic residues and amorphous carbon materials that were detected in the Raman spectra. The crystalline lattice fringes were clearly visible with a d-spacing of approximately 2.06 Å confirmed by fast Fourier transform (FFT) image (Fig. 3d) corresponding to the (111) plane of cubic diamond. Noteworthy, some forbidden reflections of (200), (222), (420) were also observed at another location on the grid as shown in Fig. S5, which can be attributed to atom defects within the cubic diamond lattice [22]. These defect-containing diamonds could be considered as intermediate products or byproducts. One could speculate that the defects could be incorporated germanium atoms since the large size of the germanium atoms would distort the crystalline structure, whereas the low Ge amount would not be sufficient to be detected in the EDX spectrum. The control experiment with a mixture of  $\text{GeI}_4$  and tetracosane without the adamantane “seed” only yielded amorphous carbon material (Fig. S6). Most likely, the cage structure of adamantane could reduce the energy barrier for diamond formation compared to alkanes as it provides a similar diamondoid structure as bulk diamond [21]. These results

indicate the important role of the molecular adamantane “seed” for nanodiamond growth. The application of  $\text{GeI}_4$  as an initiator is also essential for diamond synthesis at moderate HPHT condition as  $\text{GeI}_4$  seems to enhance the chemical reactivity of the saturated hydrocarbons. Moreover, the iodo-substituent could actively react with the unsaturated carbon bonds from the decomposed precursors, thus inhibiting the formation of graphite and stabilizing the nuclei with  $\text{sp}^3$  hybridized carbon [23,24]. We envision that the synthesis strategy reported herein opens great opportunities for the bottom-up synthesis of nanodiamond materials through molecular design of the “seed” structures.

#### 4. Conclusion

In summary, we present the first nanodiamond synthesis from adamantane and tetracosane in the presence of  $\text{GeI}_4$  that presumably serves as an initiator.  $\text{GeI}_4$  enables nanodiamond synthesis at much milder conditions *i.e.* 3.5 GPa and 500 °C, which are significantly lower than the reaction conditions during common HPHT synthesis. We envision that the combination of molecular precursors that could be further modified to impart *i.e.* heteroatom lattice defects as well as the potential initiators holds great promise for engineered growth of nanodiamonds with tailored optical properties.

#### CRedit authorship contribution statement

**Jiaxu Liang:** Conceptualization, Investigation, Data curation, Writing - original draft. **Christopher P. Ender:** Investigation. **Todd Zapata:** Investigation. **Anna Ermakova:** Investigation. **Manfred Wagner:** Conceptualization, Project administration. **Tanja Weil:** Conceptualization, Writing - review & editing, Supervision.



## Declaration of competing interest

The authors declare that they have no known competing financial interests or personal relationships that could have appeared to influence the work reported in this paper.

## Acknowledgement

The project was funded by the European Union's ERC Synergy Grant under grant agreement No. 319130 (BioQ). This project has received funding from the European Union's Horizon 2020 Research and Innovation Program under FETOPEN grant agreement no. 858149.

## Appendix A. Supplementary data

Supplementary data to this article can be found online at <https://doi.org/10.1016/j.diamond.2020.108000>.

## References

- [1] S. Kumar, M. Nehra, D. Kedia, N. Dilbaghi, K. Tankeshwar, K.H. Kim, Nanodiamonds: emerging face of future nanotechnology, *Carbon* 143 (2019) 678–699, <https://doi.org/10.1016/j.carbon.2018.11.060>.
- [2] Y. Wu, F. Jelezko, M.B. Plenio, T. Weil, Diamond quantum devices in biology, *Angew. Chem. Int. Ed.* 55 (2016) 6586–6598, <https://doi.org/10.1002/anie.201506556>.
- [3] M.H. Alkahtani, F. Alghannam, L. Jiang, A. Almethen, A.A. Rampersaud, R. Brick, C.L. Gomes, M.O. Scully, P.R. Hemmer, Fluorescent nanodiamonds: past, present, and future, *Nanophotonics* 7 (2018) 1423–1453, <https://doi.org/10.1515/nanoph-2018-0025>.
- [4] V.N. Mochalin, O. Shenderova, D. Ho, Y. Gogotsi, The properties and applications of nanodiamonds, *Nat. Nanotechnol.* 7 (2011) 11–23, <https://doi.org/10.1038/NNANO.2011.209>.
- [5] C.X. Wang, P. Liu, H. Cui, G.W. Yang, Nucleation and growth kinetics of nanocrystals formed upon pulsed-laser ablation in liquid, *Appl. Phys. Lett.* 87 (2005) 201913, <https://doi.org/10.1063/1.2132069>.
- [6] R.J. Nemanich, J.A. Carlisle, A. Hirata, K. Haenen, CVD diamond—research, applications, and challenges, *MRS Bull.* 39 (2014) 490–494, <https://doi.org/10.1557/mrs.2014.97>.
- [7] E.A. Ekimov, O.S. Kudryavtsev, A.A. Khomich, O.I. Lebedev, T.A. Dolenko, I.I. Vlasov, High-pressure synthesis of boron-doped ultrasmall diamonds from an organic compound, *Adv. Mater.* 27 (2015) 5518–5522, <https://doi.org/10.1002/adma.201502672>.
- [8] R.H. Wentorf Jr., The behavior of some carbonaceous materials at very high pressures and high temperatures, *J. Phys. Chem.* 69 (1965) 3063–3069, <https://doi.org/10.1021/j100893a041>.
- [9] F.P. Bundy, Direct conversion of graphite to diamond in static pressure apparatus, *Science* 137 (1962) 1057–1058, <https://doi.org/10.1126/science.137.3535.1057>.
- [10] H. Sumiya, Novel development of high-pressure synthetic diamonds “ultra-hard nano-polycrystalline diamonds”, *SEI Tech. Rev.* 74 (2012) 15–23 <https://global-sei.com/technology/tr/bn74/pdf/74-03.pdf>.
- [11] X. Liu, X. Jia, Z. Zhang, Y. Li, M. Hu, Z. Zhou, H. Ma, Crystal growth and characterization of diamond from carbonyl iron catalyst under high pressure and high temperature conditions, *Cryst. Growth Des.* 11 (2011) 3844–3849, <https://doi.org/10.1021/cg200387n>.
- [12] S. Sun, X. Jia, B. Yan, F. Wang, N. Chen, Y. Li, H. Ma, Synthesis and characterization of hydrogen-doped diamond under high pressure and high temperature, *CrystEngComm* 16 (2014) 2290–2297, <https://doi.org/10.1039/c3ce42385a>.
- [13] Y.N. Palyanov, I.N. Kupriyanov, A.F. Khokhryakov, Y.M. Borzdov, High-pressure crystallization and properties of diamond from magnesium-based catalysts, *CrystEngComm* 19 (2017) 4459–4475, <https://doi.org/10.1039/c7ce01083d>.
- [14] E.A. Ekimov, O.S. Kudryavtsev, N.E. Mordvinova, O.I. Lebedev, I.I. Vlasov, High-pressure synthesis of nanodiamonds from adamantane: myth or reality? *Chemnanomat* 4 (2018) 269–273, <https://doi.org/10.1002/cnma.201700349>.
- [15] M. Alkahtani, J. Lang, B. Naydenov, F. Jelezko, P. Hemmer, Growth of high-purity low-strain fluorescent nanodiamonds, *ACS Photonics* 6 (2019) 1266–1271, <https://doi.org/10.1021/acsphotonics.9b00224>.
- [16] M. Spohn, M. Alkahtani, R. Leiter, H. Qi, U. Kaiser, P. Hemmer, U. Ziener, Poly(1-vinyladamantane) as a template for nanodiamond synthesis, *ACS Appl. Nano Mater.* 1 (2018) 6073–6080, <https://doi.org/10.1021/acsnm.8b01238>.
- [17] M.A. Gebbie, H. Ishiwata, P.J. McQuadea, V. Petrak, A. Taylor, C. Freiwalde, J.E. Dahl, R.M.K. Carlson, A.A. Fokin, P.R. Schreiner, Z. Shen, M. Nesladek, N.A. Melosh, Experimental measurement of the diamond nucleation landscape reveals classical and nonclassical features, *Proc. Natl. Acad. Sci. U. S. A.* 115 (2018) 8284–8289, <https://doi.org/10.1073/pnas.1803654115>.
- [18] S.S. Lobanov, P.N. Chen, X.J. Chen, C.S. Zha, K.D. Litasov, H.K. Mao, A.F. Goncharov, Carbon precipitation from heavy hydrocarbon fluid in deep planetary interiors, *Nat. Commun.* 4 (2013) 2446, <https://doi.org/10.1038/ncomms3446>.
- [19] W.L. Huang, G.A. Otten, Cracking kinetics of crude oil and alkanes determined by diamond anvil cell-fluorescence spectroscopy pyrolysis: technique development and preliminary results, *Org. Geochem.* 32 (2001) 817–830, [https://doi.org/10.1016/S0146-6380\(01\)00038-9](https://doi.org/10.1016/S0146-6380(01)00038-9).
- [20] C. Casiraghi, F. Piazza, A.C. Ferrari, D. Grambole, J. Robertson, Bonding in hydrogenated diamond-like carbon by Raman spectroscopy, *Diam. Relat. Mater.* 14 (2005) 1098–1102, <https://doi.org/10.1016/j.diamond.2004.10.030>.
- [21] S. Park, I.I. Abate, J. Liu, C. Wang, J.E.P. Dahl, R.M.K. Carlson, L. Yang, V.B. Prakapenka, E. Greenberg, T.P. Devereaux, C. Jia, R.C. Ewing, W.L. Mao, Y. Lin, Facile diamond synthesis from lower diamondoids, *Sci. Adv.* 6 (2020) eaay9405, <https://doi.org/10.1126/sciadv.aay9405>.
- [22] D.J. Kennett, J.P. Kennett, A. West, G.J. West, T.E. Bunch, B.J. Culleton, J.M. Erlandson, S.S. Que Hee, J.R. Johnson, C. Mercer, F. Shen, M. Sellers, T.W. Stafford Jr., A. Stich, J.C. Weaver, J.H. Wittke, W.S. Wolbach, Shock-synthesized hexagonal diamonds in Younger Dryas boundary sediments, *Proc. Natl. Acad. Sci. U. S. A.* 106 (2009) 12623–12628, <https://doi.org/10.1073/pnas.0906374106>.
- [23] E.A. Ekimov, S.G. Lyapin, Y.V. Grigoriev, I.P. Zibrov, K.M. Kondrina, Size-controllable synthesis of ultrasmall diamonds from halogenated adamantanes at high static pressure, *Carbon* 150 (2019) 436–438, <https://doi.org/10.1016/j.carbon.2019.05.047>.
- [24] E.A. Ekimov, M.V. Kondrin, S.G. Lyapin, Y.V. Grigoriev, A.A. Razgulov, V.S. Krivobok, S. Gierlotka, S. Stelmakh, High-pressure synthesis and optical properties of nanodiamonds obtained from halogenated adamantanes, *Diam. Relat. Mater.* 103 (2020) 107718, <https://doi.org/10.1016/j.diamond.2020.107718>.